HNPS Advances in Nuclear Physics

Vol 22 (2014)

HNPS2014

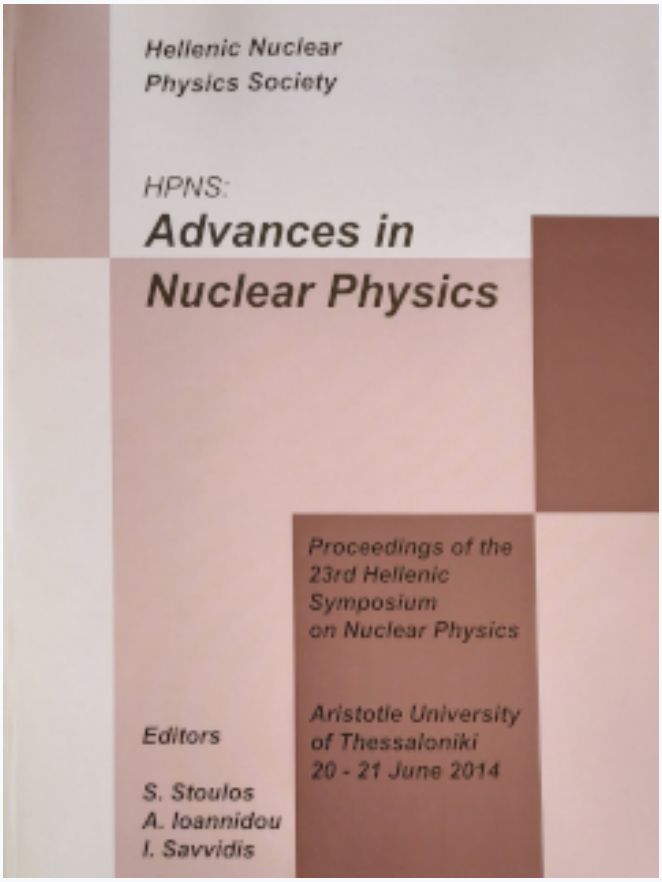

Proton capture reactions in medium-heavy nuclei relevant to p-process nucleosynthesis

V. Foteinou, M. Axiotis, A. Lagoyannis, P. Demetriou, H.-W. Becker, D. Rogalla, S. Harissopulos

doi: 10.12681/hnps.1938

Proton capture reactions in medium-heavy nuclei relevant to p-process nucleosynthesis

V. Foteinou[1], G. Provatas[1], M. Axiotis[1], A. Lagoyannis[1], P. Demetriou[1], H.-W. Becker[2], D. Rogalla[2] and S. Harissopulos[1]

[1] *Institute of Nuclear Physics, NCSR "Demokritos", 153 10 Aghia Paraskevi, Athens, Greece.*
[2] *DTL–Institut für Experimentalphysik III, Ruhr–Universität Bochum, 40781 Bochum, Germany.*

Abstract
Cross-section measurements of proton-capture reactions on Molybdenum isotopes have been performed at beam energies from 2.0 to 6.2 MeV. The cross-section data obtained in this work are compared with those predicted by theory. The latter were calculated using the latest version of the TALYS Hauser-Feshbach (HF) theory code [1] (version 1.6). In these calculations, various phenomenological and (semi)microscopic models were used for the nucleon-nucleus and the α-particle-nucleus optical model potential, the nuclear level densities and the γ-ray strength function.

Introduction

The term p-process refers to the process that describes the synthesis of the so-called *"p nuclei"*, 35 stable, proton rich nuclei which are located northwest of the valley of stability between the isotopes ^{74}Se and ^{196}Hg [2]. The formation of the p-nuclei takes place through a complicated reaction network which consists of *(γ,p)*, *(γ,n)*, *(γ,α)* and the inverse *(p,γ)*, *(n,γ)* and *(α,γ)* reactions along with *β*+ decay and Electron Capture.
There are various nucleosynthesis scenarios describing the production of the *p* nuclei however, in most cases, the theoretical and the observed abundances present significant discrepancies that necessitate the review of not only the astrophysical assumptions involved in the *p*-process modeling but also the reaction rates involved in the reaction network. Due to the huge number of reactions involved in this network *p*-nuclei abundance calculations have to rely on the predictions of the Hauser-Feshbach (HF) theory. It is therefore necessary to check the reliability of the nuclear parameters entering the HF calculations, i.e., the nucleon-nucleus and the α-particle-nucleus Optical Model Potential (OMP), the Nuclear Level Densities (NLD) and the γ-ray Strength Function (γSF).
The present work focuses on systematic cross-section measurements of *p*-capture reactions on Molybdenum isotopes. The measurements were carried out at beam energies which are convenient for the qualification and optimization of the proton-nucleus optical potential.

Experimental procedures

The measurements were carried out at the Dynamitron-Tandem-Laboratorium (DTL) of the Ruhr-Universität Bochum in Germany. The cross sections of the ^{92}Mo(p,γ)^{93}Tc, ^{94}Mo(p,γ)^{95}Tc, ^{96}Mo(p,γ)^{97}Tc, ^{97}Mo(p,γ)^{98}Tc, ^{98}Mo(p,γ)^{99}Tc and ^{100}Mo(p,γ)^{101}Tc reactions were determined at beam energies between 2.0 and 6.2 MeV. The 4π γ-summing method [3] was used in all cases. The experimental setup consisted of a 12″×12″ NaI detector covering a solid angle of 98% of 4π for photons emitted at its center [4]. The energy resolution of the detector was almost 2% for γ rays of energy E_γ=10 MeV.
During the measurements the target was placed on a Ta holder mounted at the center of the NaI detector. To ensure that no deterioration of the targets occurred, the latter were air cooled during the measurements. Aiming to the suppression of the induced background, two thick Au layers were mounted on the back of the targets. All targets used were prepared by rolling highly isotopically enriched material in the form of self-supporting foils. The thicknesses of the targets (252-1123μgr/cm^2) were determined at the Tandem Laboratory of NCSR "Demokritos" by applying the Rutherford Backscattering Spectroscopy (RBS) technique. The energy straggling of each target was calculated by simulation using the SRIM code [5]. The isotopic abundances were provided by the manufacturers.

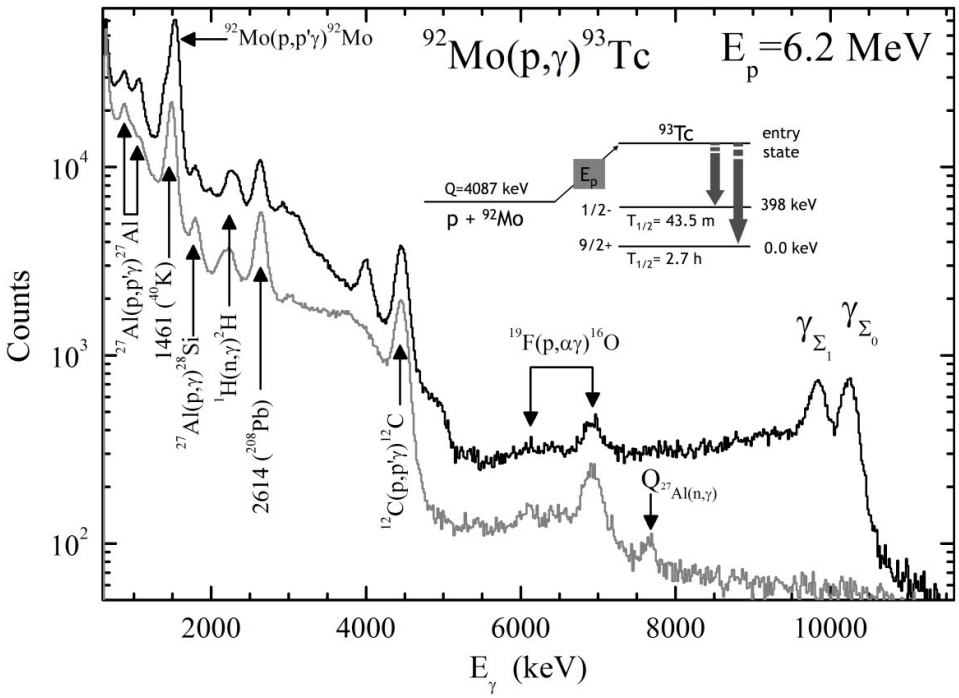

Fig. 1: Typical spectrum of the ^{92}Mo(p,γ)^{93}Tc reaction measured at E$_p$=6.2 MeV with a 4π-summing detector. A metastable state of the produced nucleus ^{93}Tc at 392 keV results in the second peak γ_{Σ_1}.

A typical spectrum of the ^{92}Mo(p,γ)^{93}Tc reaction measured by the summing crystal at E$_p$=6.2MeV is presented in Fig. 1. Apart from the γ_{Σ_0} summing peak, which corresponds to the sum of all the transitions from the entry to the ground state, a second sum peak, labeled as γ_{Σ_1}, is observed. This second peak results from all the cascades depopulating the entry state to the 1st excited state of the produced nucleus ^{93}Tc at 392 keV [6]. The latter has a half life equal to 43.5 m, much greater than the response time of the detector. Apart from the aforementioned sum peaks, several peaks can be observed on the spectrum originating from reactions of the beam with the target, the holder or with target impurities. Peaks from natural background radiation are also observed at 1461 and 2614 keV. Furthermore, the ideally isolated and background free sum peak is not the case, as seen in Fig. 1 where the sum peaks lie on a Compton continuum arising from photons escaping the crystal.

Data analysis and results

The total cross section σ_T of a capture reaction measured by means of the 4π γ-summing method is obtained by

$$\sigma_T = \frac{A}{N_A \xi} Y$$

where A is the atomic weight of the target given in amu, N_A the Avogadro's number in nuclei/mol, ξ the thickness of the target in gr/cm^2 and Y the number of the produced nuclei per beam particle. The latter is equal to the corrected for the dead time and normalized to the beam current and the efficiency intensity of the sum peak.

The total cross sections obtained in this work for the ^{92}Mo(p,γ)^{93}Tc, ^{94}Mo(p,γ)^{95}Tc, ^{96}Mo(p,γ)^{97}Tc, ^{97}Mo(p,γ)^{98}Tc, ^{98}Mo(p,γ)^{99}Tc and ^{100}Mo(p,γ)^{101}Tc reactions range between 4 and 6500 μb with a total error less than 22% in all cases apart from the ^{97}Mo(p,γ)^{98}Tc reaction where it varied between 25% and 60%. Apart from the statistical errors, uncertainties due to the thicknesses of the targets (7%), the beam current (3%) and the detector efficiency (11-20%) have also been considered. The experimental data obtained here for the ^{100}Mo(p,γ)^{101}Tc reaction are presented in Fig. 2. All cross sections were corrected for the electron screening effect as described in [7] and [8].

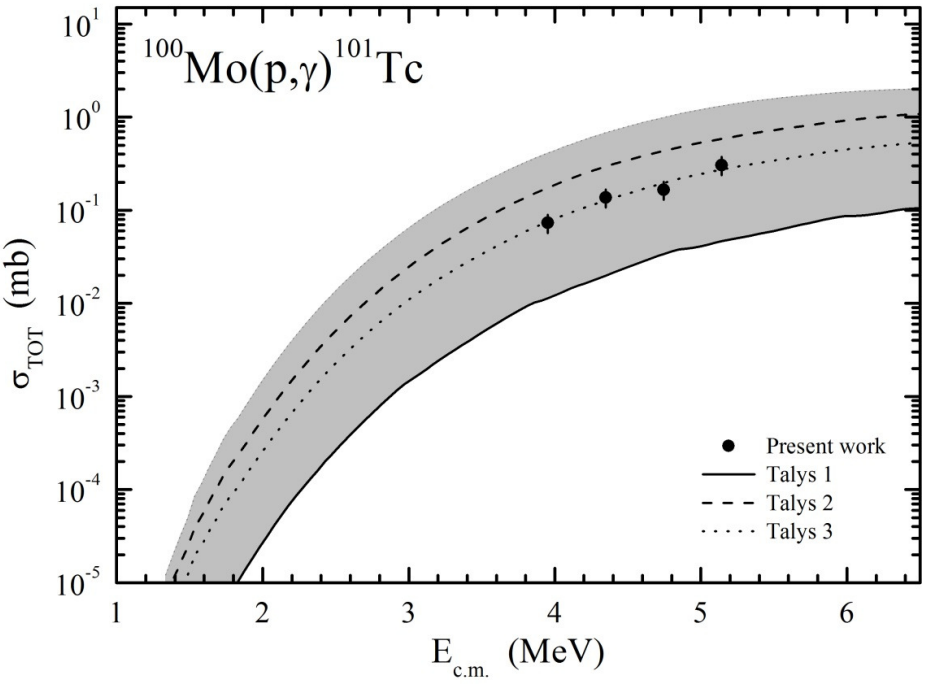

Fig. 2: Total cross sections of the ^{100}Mo(p,γ)^{101}Tc reaction. The dots correspond to the experimental data obtained in this work whereas the solid, dashed and dotted lines labeled as TALYS 1, 2 and 3 correspond to HF predictions calculated considering the three combinations of the nOMP, αOMP, NLD and γSF parameters that are described in the text. The shaded areas represent the theory limits, estimated by taking into account all the available models included in version 1.6 of TALYS.

The HF calculations presented in this report were performed using the version 1.6 of the statistical code TALYS [1]. In this code the nucleon-nucleus Optical Model Potential (nOMP), the α-particle-nucleus Optical Model Potential (αOMP), the Nuclear Level Densities (NLDs) and the γ-ray Strength Function (γSF) can be determined according to both phenomenological and microscopic models. Among the models that are implemented in TALYS for the aforementioned parameters, we took into consideration three basic combinations, one purely phenomenological and two semi-microscopic. The phenomenological one (TALYS 1) consists of the nucleon-nucleus OMP by Koning and Delaroche [9], the Constant Temperature Fermi Gas model by TALYS group for the Nuclear Level Densities [1] and the Generalized Lorentzian model by Kopecky and Uhl [10] for the γ-ray Strength Function. The two semi-microscopic combinations, namely TALYS 2 and TALYS 3, are composed of the Bauge, Delaroche and Girod nOMP [11] and NLD, γSF models based on Hartree-Fock-BCS [12,13] (TALYS 2) and Hartree-Fock-Bogolyubov [13,14,15] (TALYS 3) calculations. For all three combinations we have considered the phenomenological folding approach of Watanabe [16] in the Koning-Delaroche potential [9] for the α-particle-nucleus optical potential. The shaded areas in Fig. 2 represent the theory limits estimated by taking into account all the available models of the nOMP, αOMP, NLD and γSF parameters implemented in TALYS. As can be observed in Fig. 2 the experimental data are in very good agreement with the predictions of theory and particularly with the semi-microscopic combination TALYS 3. Such a good agreement was observed between the experimental data and several theoretical calculations for every reaction. However there is no unique combination capable of reproducing all cases.

Conclusions

In the present work the total cross sections of the ^{92}Mo(p,γ)^{93}Tc, ^{94}Mo(p,γ)^{95}Tc, ^{96}Mo(p,γ)^{97}Tc, ^{97}Mo(p,γ)^{98}Tc, ^{98}Mo(p,γ)^{99}Tc and ^{100}Mo(p,γ)^{101}Tc reactions were determined in astrophysically relevant energy ranges applying the 4π γ-summing method. All experimental data obtained in this

work were in good agreement with the predictions of the Hauser-Feshbach theory. The theoretical calculations were performed using the version 1.6 of the statistical code TALYS. For these calculations various models for the nucleon-OMP, the α-particle-OMP, the NLD and the γSF nuclear parameters were taken into account.

References

1. A.J. Koning, S.Hilaire and M.C. Duijvestijn, "TALYS-1.4", Proceedings of the International Conference on Nuclear Data for Science and Technology, April 22-27, 2007, Nice, France, editors O. Bersillon, F. Gunsing, E. Bauge, R. Jacqmin, and S.Leray, EDP Sciences, 2008, p. 211-214.
2. M. Arnould and S. Goriely, Phys. Rev. 384 (2003) 1-84.
3. A. Spyrou, H.-W. Becker, A. Lagoyannis, S. Harissopulos, and C. Rolfs, Phys. Rev. C 76, 015802 (2007).
4. N. Piel, W.H. Schulte, M. Berheide, H.W. Becker, L. Borucki, C. Grama, M. Mehrhoff, C. Rolfs, NIM B 118, 186 189 (1996).
5. J. Ziegler, J. Biersack, and U. Littmark, The Stopping and Range of Ions in Solids, Pergamon Press (1985).
6. R. B. Firestone, V. S. Shirley, C. M. Baglin, J. Zipkin, and S. Y. F. Chu, Table of Isotopes. Wiley-Interscience (1996).
7. C. E. Rolfs and W. S. Rodney, Cauldrons in the Cosmos (1988).
8. K. U. Kettner, H. W. Becker, F. Strieder, C. Rolfs Jour. of Phys. G 32, 4, 489 (2006).
9. A. Koning and J. Delaroche, Nuclear Physics A 713, no. 3-4, pp. 231-310 (2003).
10. J. Kopecky and M. Uhl Phys. Rev. C, vol. 41, p. 1941(1990).
11. E. Bauge, J. P. Delaroche, and M. Girod, Phys. Rev. C, vol. 63, p. 024607 (2001).
12. P. Demetriou and S. Goriely, Nuclear Physics A 695, no. 1-2, pp. 95-108 (2001).
13. E. Khan, S. Goriely, D. Allard, E. Parizot, T. Suomijarvi, A. Koning, S. Hilaire, and M. Duijvestijn, Astropart. Phys. 23, p. 191, 2005.
14. S. Goriely, S. Hilaire, and A. J. Koning, Phys. Rev. C 78, 064307 (2008).
15. R. Capote, M. Herman, P. Obloinsk, P. Young, S. Goriely, T. Belgya, A. Ignatyuk, A. Koning, S. Hilaire, V. Plujko, M. Avrigeanu, O. Bersillon, M. Chadwick, T. Fukahori, Z. Ge, Y. Han, S. Kailas, J. Kopecky, V. Maslov, G. Reffo, M. Sin, E. Soukhovitskii, and P. Talou, Nuclear Data Sheets, vol. 110, no. 12, p. 3107 (2009).
16. S. Watanabe, Nuclear Physics, vol. 8, no. 0, pp. 484-492 (1958).